Proceedings of the 29th International Conference on Ocean, Offshore and Arctic Engineering
OMAE2010
June 6-11, 2010, Shanghai, China

OMAE2010-20891

NON-LINEAR INITIALIZATION IN THREE-DIMENSIONAL HIGH ORDER SPECTRA DETERMINISTIC SEA STATE MODELING

Yves L. Perignon
LMF-ECN, Nantes, France
Actimar, Brest, France
Yves.perignon@ec-nantes.fr

Felicien Bonnefoy, Pierre Ferrant, Guillaume Ducrozet
Laboratoire de Mécanique des Fluides - UMR 6598
Ecole Centrale de Nantes
Nantes, France

ABSTRACT

This study deals with the initialization of three-dimensional wave field computations. We carry out such simulations with an HOS model developed at LMF-ECN since 2002 and based on the work of West et al. (1987) and Dommermuth & Yue(1987). In such models, initial conditions for three-dimensional realistic sea state computation are obtained by linearly distributing energy density spectrum. This however implies a relaxation of the non-linear effects as proposed by Dommermuth(2000) for bi-dimensional monochromatic wave train and Tanaka(2001), over several tenths of wave periods. The present work tests those former initialization methods and exposes an alternative initialization based on a non-linear three-dimensional approach. Non-linear interaction processes are both accounted in the spectra of elevation and potential of velocity, in accordance with the formulation of Dalzell(1999) at second order in wave steepness. Non-linear energy calculation is then addressed and the efficiency of the methods as well as their possible impact on properties and statistics of the wave field are investigated.

INTRODUCTION

Deterministic sea state modeling is a key capability for many activities and their validation, safety, observation or forecasting. Characterizing a sea state implies to consider a superposition of high number of component waves with various amplitudes, frequencies, wave length and directions of propagation, interacting non-linearly with each other. For this purpose, we employ the High-Order Spectral (HOS hereinafter) method developed at ECN for various purposes (see Blondel et al.(2008a,b), Bonnefoy et al.(2009)). If the physics of propagative problem are quite well theorized, setting up proper initial conditions for any realistic sea state modeling may remain a difficult task. Unreal high frequency modes are generated when non-linear progressive waves are initialized using linear conditions. Solution generally used is either to allow a sufficient relaxation time for unreal mode to disappear [Tanaka(01)] or to implement a relaxation procedure [Dommermuth(00)]. Tanaka considered the spectrum of surface elevation and velocity potential verifying the linear JONSWAP distribution and showed the non-linear HOS computation implied a period of relaxation for non-linear energy transfer to occur. This was achieved after a relaxation time of about a few tens of characteristic periods. Dommermuth added to the linear initialization an adjustment procedure to allow natural development of non-linear self-wave and wave-wave interactions. This however implied a period of relaxation of a few tens of characteristic periods.

The objective here is to test comparatively a non-linear tridimensional initialization to a second order in wave steepness (employed in bidimensional wave field by Blondel et al.(08)) with both previous methods and to estimate the impact of initialization on the statistics of wave field.

1. FUNDAMENTALS

1. High Order Spectral model formalism

We consider a fluid domain of dimensions defined in a Cartesian system $(\mathbf{x},\vec{z})$. A potential of velocity $\varphi(\mathbf{x},z,t)$ is defined so as $\mathbf{V}(\mathbf{x},z,t)=\vec{\nabla}\varphi(\mathbf{x},z,t)$ assuming irrotational motion. In this study the fluid domain is assimilated to a deep-water oceanic domain. Its frontiers being defined as periodic the domain might be assimilated as infinite.

Expressing the conservation of momentum and kinematic condition at the free surface $z=\eta$ following Dommermuth and West et al., the system can be defined as :

$$\frac{\partial \varphi_s}{\partial t} = -g\eta - \frac{1}{2}\left|\nabla\varphi_s\right|^2 + \frac{1}{2}\left(1+\left|\nabla\eta\right|^2\right)W^2 - \frac{p_a}{\rho_w} \tag{1}$$

$$\frac{\partial \eta}{\partial t} = \left(1 + \left|\nabla \eta\right|^2\right) W - \nabla \varphi_s . \nabla \eta \qquad (2)$$

with $\varphi_s(\mathbf{x},t) = \varphi(\mathbf{x}, z = \eta, t)$ the potential of velocity expressed at $z = \eta$ the free surface elevation, $\frac{\partial \varphi}{\partial z} = W$ the vertical velocity at the free surface, p_a the atmospheric pressure, and ρ_w the water density. Spatial horizontal derivatives are determined analytically expressing surface elevation and surface potential on an Fourier basis such as :

$$\eta(\mathbf{x},\mathrm{t}) = \sum_{n=-\infty}^{+\infty} \sum_{p=-\infty}^{+\infty} A_{np}^{\eta}(t) e^{ik_{x_n} x} e^{ik_{y_p} y} \qquad (3)$$

$$\varphi_s(\mathbf{x},\mathrm{t}) = \sum_{n=-\infty}^{+\infty} \sum_{p=-\infty}^{+\infty} A_{np}^{\varphi_s}(t) e^{ik_{x_n} x} e^{ik_{y_p} y} \qquad (4)$$

The Fourier basis is determined by the Cartesian system in wave number, k_{x_n} and k_{y_p} being defined as $k_{x_n} = \frac{n\pi}{L_x}$ and $k_{y_p} = \frac{p\pi}{L_y}$.

Equations (1) and **(2)** allow to advance η and φ_s in time through a Runge-Kutta scheme. The only variable remaining unknown W is determined using decomposition in order of power of η and a Taylor development of φ around $z = 0$ to an order M :

$$W(\mathbf{x},\mathrm{t}) = \sum_{m=1}^{+\infty} W^{(m)}(\mathbf{x},t) \qquad (5)$$

and

$$W^{(m)}(\mathbf{x},\eta,t) = \sum_{k=0}^{+\infty} \frac{\eta^k}{k!} \frac{\partial^{k+1} \varphi^{(m-k)}}{\partial z^{k+1}}(\mathbf{x},0,t) \qquad (6)$$

where the $\varphi^{(m)}$ components of the potential are obtained by solving the Dirichlet problem of the free surface [see Dommermuth Yue(87) and West et al.(87)].

2. *Initial conditions*

Setting initial conditions is a crucial task in the process of realistic sea state modeling. Common use is to consider a distribution of density of energy and to assign η and φ_s consistently. Taking a distribution of density of energy such as JONSWAP :

$$\Phi(\omega) = \Psi(\omega) G(\theta) \qquad (7)$$

with :

$$\Psi(\omega) = \alpha g^2 \omega^{-5} \exp\left(-\frac{5\omega_p^4}{4\omega^4}\right) \gamma^{\exp\left[-(\omega-\omega_p)^2 / 2\sigma^2\omega_p^2\right]} \qquad (8)$$

The JONSWAP formulation corresponds to :

$$\alpha = 3.279E, \quad \gamma = 3.3, \quad \sigma = \begin{cases} 0.07 & (\omega < 1) \\ 0.09 & (\omega > 1) \end{cases} \qquad (9)$$

and $G(\theta)$ the function of angular repartition :

$$G(\theta) = \begin{cases} \frac{1}{\beta} \cos^2\left(\frac{\pi\theta}{2\beta}\right), & |\theta| \le \beta \\ 0, & |\theta| > \beta \end{cases} \qquad (10)$$

Surface elevation and potential are then related to the distribution of energy through their modal amplitude:

$$A^{\eta}(\mathbf{k}) = \sqrt{\frac{g}{\omega_{\mathbf{k}}^3} \Phi(\omega_{\mathbf{k}}) \Delta k_x \Delta k_y}\; e^{i\phi} \qquad (11)$$

and:

$$A^{\eta}(\mathbf{k}) = -\frac{ig}{\omega_{\mathbf{k}}} \sqrt{\frac{g}{\omega_{\mathbf{k}}^3} \Phi(\omega_{\mathbf{k}}) \Delta k_x \Delta k_y}\; e^{i\phi} \qquad (12)$$

where ϕ is the random phase of the complex modal component, Δk_x and Δk_y the discretization steps in the spectral domain.

We consider here a second order non-linear initialization thanks to the formulation of Dalzell(99) following Longuet-Higgins(62) and generalized to a discrete spectrum of elevation and potential of velocity. Expressions are given for a case of infinite depth.

$$\eta(\mathbf{x}) = \eta^{(1)} + \eta_s + \eta_+ + \eta_- \qquad (13)$$

The first term corresponds to the linear contribution, the second to the Stokes interaction of a component on itself and the last ones to the additive contributions within the spectrum. The first order elevation is written as follows :

$$\eta_1 = \sum_{n=1}^{N} \sum_{p=1}^{P} A_{np}^{\eta} e^{ik_{x_n} x} e^{ik_{y_p} y} \qquad (14)$$

where N and P are respectively the number of modes along $\vec{k}_x$ and $\vec{k}_y$ as well as the dimensions of the spatial discrete grid along $\vec{x}$ and $\vec{y}$.

The second order components are expressed by :

$$\eta_s = \sum_{n=1}^{N} \sum_{p=1}^{P} \frac{{A_{np}^{\eta}}^2 k_{np}}{2} e^{i2k_{x_n} x} e^{i2k_{y_p} y} \qquad (15)$$

$$\eta_+ = \sum_{n=1}^{N} \sum_{p=1}^{P} \sum_{i=n+1}^{N} \sum_{j=p+1}^{P} A_{np}^{\eta} A_{ij}^{\eta} B_+(\mathbf{k_{np}}, \mathbf{k_{ij}}) e^{i\left(k_{x_n} + k_{x_i}\right)x} e^{i\left(k_{y_p} + k_{y_j}\right)y} \qquad (16)$$

$$\eta_- = \sum_{n=1}^{N}\sum_{p=1}^{P}\sum_{i=n+1}^{N}\sum_{j=p+1}^{P} A_{np}^{\eta}\, A_{ij}^{\eta}\, B_-\left(\mathbf{k_{np}},\mathbf{k_{ij}}\right) e^{i\left(k_{x_n}-k_{x_i}\right)x} e^{i\left(k_{y_p}-k_{y_j}\right)y} \tag{17}$$

Those are functions of sum and differences contributions B_+ and B_-, given in appendix A.

The surface potential at second order is obtained by a Stokes development and a Taylor expansion around $z=0$:

$$\varphi_s(\mathbf{x}) = \varphi^{(1)}(\mathbf{x},z=0) + \varphi^{(2)}(\mathbf{x},z=0) + \eta^{(1)} \frac{\partial \varphi^{(1)}(\mathbf{x},z=0)}{\partial z} \tag{18}$$

The first order potential is expressed in Dalzell as:

$$\varphi^{(1)}(\mathbf{x},z=0) = \sum_{n=1}^{N}\sum_{p=1}^{P} i\, A_{np}^{\eta} \frac{g}{\omega_{np}} e^{ik_{x_n}x} e^{ik_{y_p}y} \tag{19}$$

and the second order by :

$$\begin{aligned}\varphi^{(2)}(\mathbf{x},z=0) = & \sum_{n=1}^{N}\sum_{p=1}^{P}\sum_{i=n+1}^{N}\sum_{j=p+1}^{P} i\, A_{np}^{\eta}\, A_{ij}^{\eta}\, A_+\left(\mathbf{k_{np}},\mathbf{k_{ij}}\right) e^{i\left(k_{x_n}+k_{x_i}\right)x} e^{i\left(k_{y_p}+k_{y_j}\right)y} \\ & + \sum_{n=1}^{N}\sum_{p=1}^{P}\sum_{i=n+1}^{N}\sum_{j=p+1}^{P} i\, A_{np}^{\eta}\, A_{ij}^{\eta}\, A_-\left(\mathbf{k_{np}},\mathbf{k_{ij}}\right) e^{i\left(k_{x_n}-k_{x_i}\right)x} e^{i\left(k_{y_p}-k_{y_j}\right)y}\end{aligned} \tag{20}$$

Sum and differences contributions of wave numbers A_+ and A_- are given in appendix A.

3. *Non-linear relaxation*

Spurious wave damping as expressed by Dommermuth(00) through a relaxation coefficient for non-linearities to be taken progressively into account has also been implemented to compare the performances of the different methods. Parameters Ta and n control the relaxation of the non-linear terms F and G such as:

$$\frac{\partial \varphi_s}{\partial t} = -g\eta + G\left(1 - e^{-\left(t/T_a\right)^n}\right) \tag{21}$$

$$\frac{\partial \eta}{\partial t} = W + F\left(1 - e^{-\left(t/T_a\right)^n}\right) \tag{22}$$

This however implies that proper relaxation requires time or inversely that quick initialization implies poor accuracy.

2. NUMERICAL RESULTS

1. *Second order test case*

We consider here the theoretical test case of propagation for regular Stokes wave. An ideal time-domain second order solver is able to propagate through time and space a stable Stokes solution such as:

$$\begin{cases} \eta(x,t) = a\cos(kx-\omega t) + \dfrac{1}{2} ka^2 \cos\left(2\left(kx-\omega t\right)\right) \\ \varphi(x,t) = a\sin(kx-\omega t) \end{cases} \tag{23}$$

When initialized linearly, a non-linear solver will combine the proper non-linear solution (free and bound mode) to a free standing mode at $2k$, with a pulsation $\omega(2k) \neq 2\omega(k)$, validating the initial conditions:

$$\eta(x,t=0) = a\cos(kx) + \frac{1}{2}ka^2\cos(2kx) - \frac{1}{2}ka^2\cos(2kx) \tag{24}$$

This is indeed equivalent to the combination of a linear free mode and a spurious non-linear one:

$$\eta(x,t) = a\cos(kx-\omega_k t) + \frac{1}{2}ka^2\left[\cos\left(2kx-2\omega_k t\right) - \cos(2kx)\cos(\omega_{2k}t)\right] \tag{25}$$

The non-linear solver (HOS) we will use in this section is not strictly equivalent, when set with M=2, to the ideal second order solver discussed above. Indeed, second order in development of the vertical velocity in HOS does not properly correspond to a second order in wave steepness, as HOS cinematic boundary conditions are expressed at free surface $z=\eta$ when Dalzell development of nonlinearities to a second order (i.e. Stokes waves in case of regular waves) is expressed around the mean lever $z=0$. As the difference implied is greater than two in term of non-linear order (and then lower in magnitude), it was interesting to test comparatively linear and non-linear initializations and their impact on stability in HOS M=2.

Initialization is compared for an initial Airy linear wave solution, an initial Airy linear simulation with non-linear relaxation as expressed by Dommermuth(00) and a Stokes wave. Their propagation is performed with HOS M=2, and the amplitude is taken so as to consider a wave steepness given by $ka=0.1$.

The amplitude of the second order component (i.e. at $2k_p$), shows the influence of spurious modes with amplitude about 2 times the theoretic second order amplitude, in the case of linear initialization (Figure 1). Oscillations up to ±4% are also present in case of Dalzell initialization. Those are indeed part of the difference of non-linear development in HOS M=2, and their magnitude remains weak compared to the standing mode of the linear case. Spurious modes at higher harmonics are also present but apparently lower in the case of second order non-linear initialization.

This is tested here for the theoretic test case of regular waves. For such cases, non-linear initialization enables to reach initially the same accuracy as a relaxation process with Ta = 2 to 3 Tp, and an efficient time of relaxation of about 4 to 6 Tp (Figure 2).

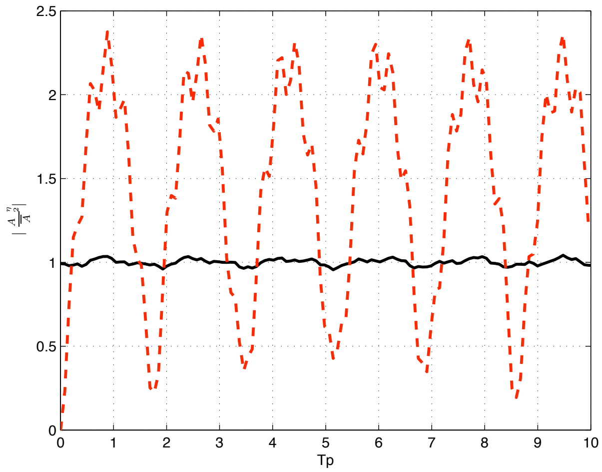

Figure 1 - Theoretic test case : amplitude of the second mode of η through time for linear (red dotted) and non-linear (black continuous) initialization in a HOS M=2 computation (both normalized by mean value of the second order mode amplitude).

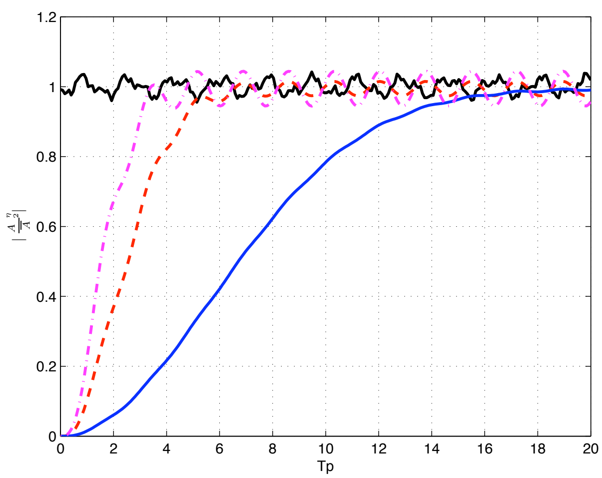

Figure 2 - Comparison of the amplitudes of the second mode of surface elevation for non-linear (black continuous) and linear with relaxation of non-linearities (n=2, Ta=2 (cyan dash-dotted), Ta=3 (red dashed), Ta=8 (blue continuous)). All normalized by the mean value of the second order mode amplitude.

It then appears that second order non-linear initialization following Dalzell's formulation provides an immediate quite stable estimation of the non-linearities at $k = 2k_p$. For such a theoretic test case Dommermuth initialization enables however a more accurate estimation of the whole range of non-linear harmonic components although it will require a significant relaxation period [Dommermuth(00)].

2. *Realistic continuous spectrum*

The main goal of this study remains the evaluation of performances for various initialization methods for continuous spectrum of realistic sea-states. This is tested now on various distribution laws for the spectrum of density of energy. So as to compare coherently those different initializations, non-linear energy is taken as the physical quantity of reference. Its expression is given by:

$$E = \frac{1}{2}\iint \phi \frac{\partial \eta}{\partial t} d\mathbf{x} + \frac{1}{2}\iint \eta^2 d\mathbf{x} \tag{26}$$

Its calculation is included in a convergence loop, so that the non-linear energy of the initial state corresponds to the same prescribed energy, independently of the initialization methods. In fact, in case of nonlinear initialization, the energy of linear free components and second order bound components need to be equivalent to the energy of the initial linear sea state.

2.1. Numerical details

Modeling a realistic sea state implies to take into account directional nonlinear interactions. The nonlinear order is set up to an order M=3 and enables to consider properly up to nonlinear Hasselmann(62)'s transfers. HOS simulations on spatial grid size of about 768 by 375 nodes are performed on durations up to $100T_p$. Spatial domain is chosen square so that it length is equal to $50\lambda_p$, setting the peak wave number at the 50th component. Total energy is set so as to verify a pseudo steepness parameter such as $\varepsilon = H_s k_p = 0.1$. Various distributions laws with the same initial random phase draw were tested in term of efficiency for three types of initialization: linear distribution, Dommermuth nonlinear relaxation, and second order nonlinear initialization, which is assumed to make up a first step toward a fully nonlinear relaxed sea state. A comparative review of their performances is then achieved.

2.2. Nonlinear transfers

Following Tanaka(01), the directional nonlinear transfer through time are evaluated studying the time variations of the density of spectral energy given by :

$$T_E(k_x, k_y) = \frac{E_{k_x,k_y}(t_2) - E_{k_x,k_y}(t_1)}{\Delta t} \tag{27}$$

with:

$$E(k_x, k_y) = \frac{1}{2\,\Delta k_x \Delta k_y}\left|A^{\eta}_{k_x,k_y}\right|^2 \tag{28}$$

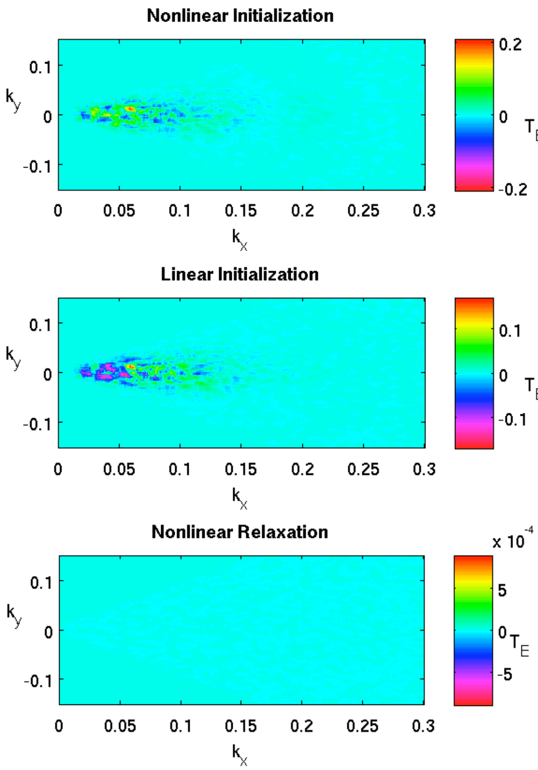

Figure 3 - Transfer in the spectral density spectrum between initial state t=0 and t=1Tp for three different initialization procedures.

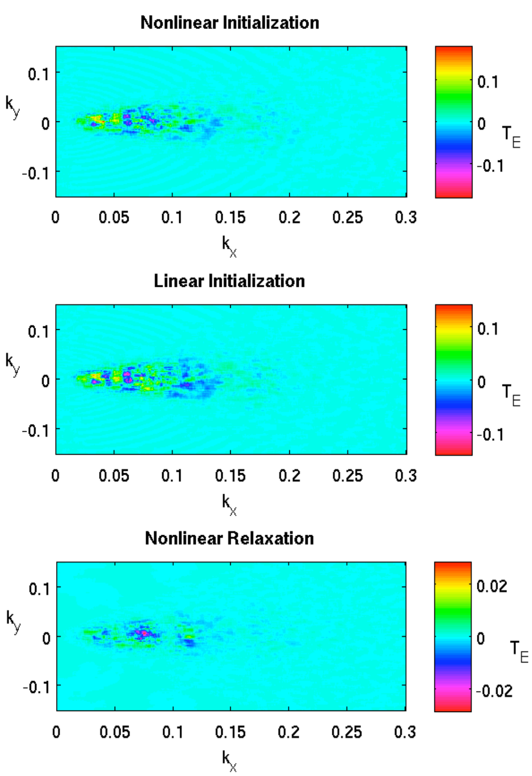

Figure 4 – Transfer in the spectral density Spectrum between t = 5Tp and t=6Tp.

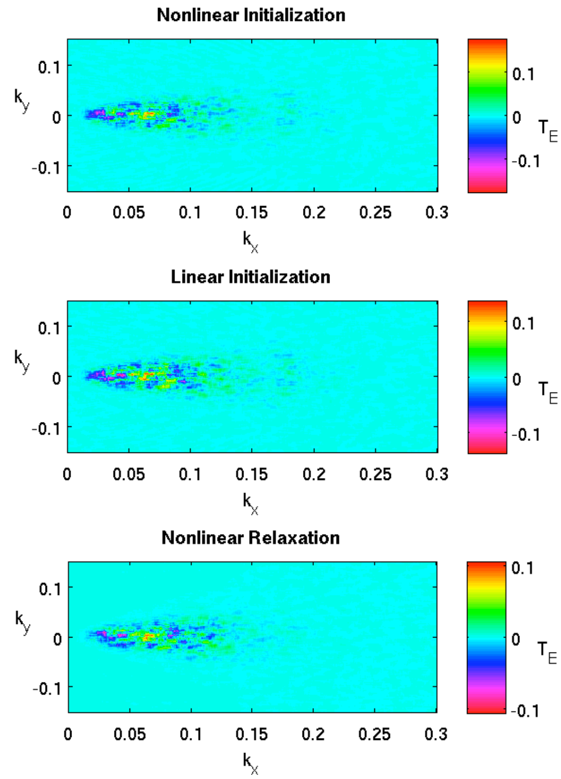

Figure 5 - Transfer in the spectral density spectrum between t=10 and t=11Tp.

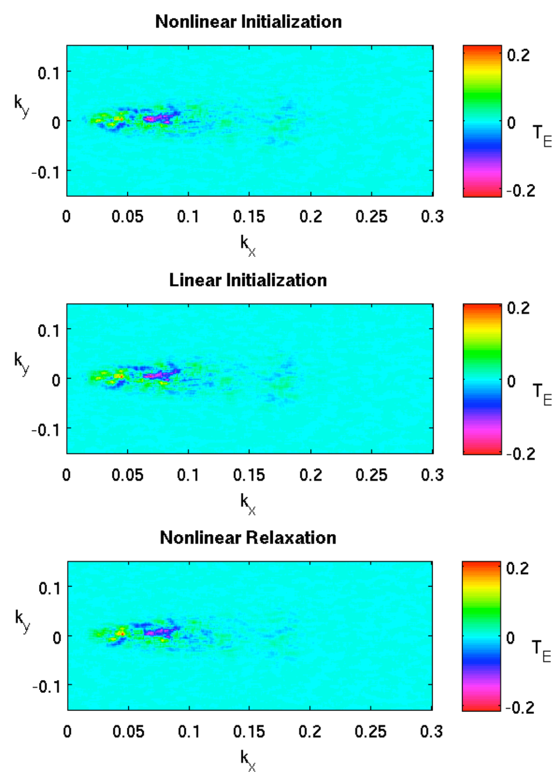

Figure 6 - Transfer in the spectral density spectrum between t=20 Tp and t=21Tp

the spectral density of energy function of the complex modal amplitude. Such transfers are plotted in Figure 3 to 6 for the different initializations.

The integrated transfer through direction [Tanaka(01)] will also be a valuable variable to study :

$$T_E(k) = \frac{E_k(t_2) - E_k(t_1)}{\Delta t} \tag{29}$$

with:

$$E(k) = \int_{\|\mathbf{k_x}+\mathbf{k_y}\|=k} k\, E(k_x, k_y)\, d\theta \tag{30}$$

Considering the linear nature of the spectral density, it has to be pointed out that it is not evaluated here to assess any energetic quantity, but to provide a valuator of the nonlinear evolutions among the amplitude spectrum. Whereas Tanaka used this quantity over few tens of characteristic periods in order to compare computed transfers to Hasselmann's theory, it was chosen here to evaluate the transfer over one characteristic period. This way, the valuator is assumed to capture the non-linear adjustments at the basis of initial set up. A moving average is used over ten by ten squares grid points in the spectral domain to filter the high frequency spectral variations. Considering the high number of frequencies, the moving average acts as a multiple initial phase draw for the various components. The major trend in term of nonlinear transfers is then made more obvious. The figures presented here show consistently the same initial phase draw for all three different methods of initialization.

Common JONSWAP sea states [Equation **(9)**] are used as initial conditions. The nonlinear relaxation as expressed by Dommermuth allows to take gradually into account the nonlinear terms. The first time steps are then predominantly linear for this initialization.

2.3. Results

Bidimensional expression of the nonlinear transfers gives a first qualitative sight of the processes at stake. Those nonlinear transfers appear to remain low up to five times the peak period (Figure 3 and 4). Linear and nonlinear initializations show slight differences over the first time steps (Figure 3), but their qualitative specifications tend to reduce comparatively through time (Figure 4 and **5**). After about twenty characteristic periods, all three methods of relaxation seem to produce quite similar transfers (Figure 6).

This is also verified through the study of transfers for the integrated spectral density and provides a more quantitative As shown by Tanaka, relaxation of the nonlinear set up occurs after an order of one tens of time the characteristic period. By relaxed sea state, it is implied that free wave components are accompanied by the appropriate corresponding bound waves. During relaxation, progressive waves are observed in the spectral space (Figure 4). This is consistent with what was expressed in paragraph 1 for the regular sea state as it reveals the presence of spurious standing components which are now transient. Indeed, the standing modes are dissipated through third order nonlinearities (i.e. four waves resonant interactions). The main differences occur at the first time steps (Figure 7 and 8), and after the 10 Tp evaluated relaxation period the correlation between quantities of transfer for the three methods of initialization becomes significant (Figure 9 and 10).

2.4. Statistics

The influence of initialization is also sensible in term of statistics of the sea states. The density of probability of surface elevation is computed for each case and compared to distributions of reference.

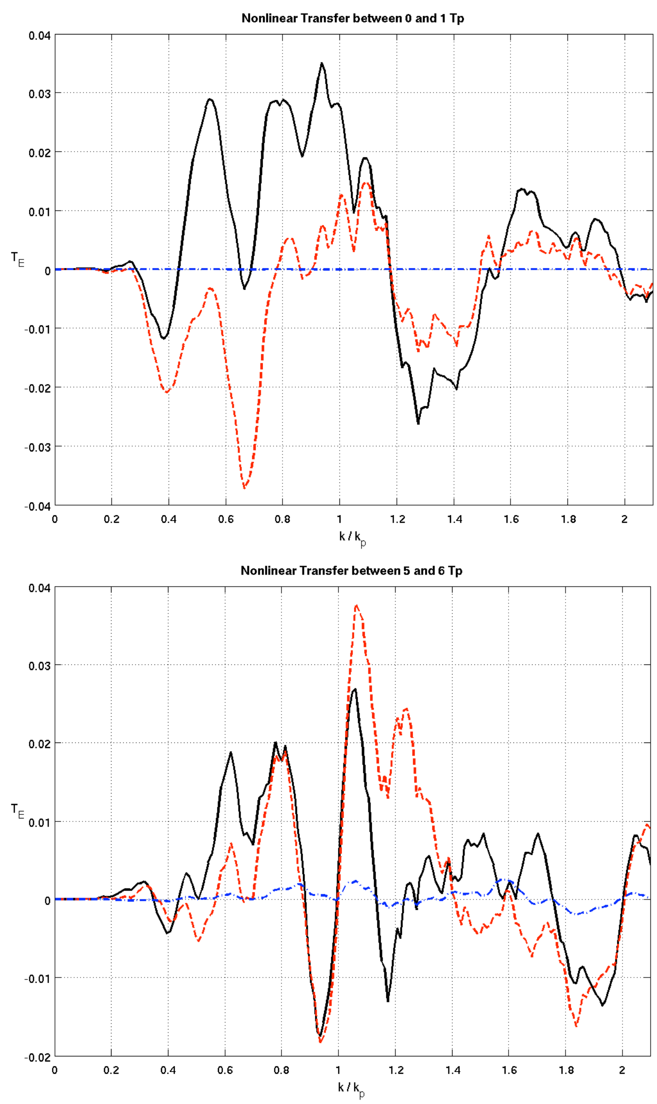

Figure 7 and Figure 8 - Integrated nonlinear transfers for second order non linear initialisation (black continuous), linear (red dashed) and relaxed (blue dash -dotted) initialization between 0 and 1 Tp and 5 and 6 Tp.

A linear distribution is assumed to follow a Gaussian repartition [Longuet-Higgins(52)] under the form:

$$f_G(\eta) = \frac{1}{\sigma\sqrt{2\pi}} \exp\left[-\frac{(\eta-\mu)^2}{2\sigma^2}\right] \tag{31}$$

with σ and μ the standard deviation and mean of the data set, respectively. Many formulations for probability distribution of nonlinear sea states are available, and among them we chose to consider Tayfun(80)'s formulation for non linear stokes expansion to the second order:

$$f_T(\eta) = \frac{1-7\sigma^2/8}{\sqrt{2\pi\left(1+3G+2G^2\right)}} \exp\left[-\frac{G^2}{2\sigma^2}\right] \tag{32}$$

$$G = \sqrt{1+2\eta} - 1 \tag{33}$$

The comparison to computed repartitions of η is then very sensible to the number of nodes on the spatial grid of computation. The noisy repartitions are generally filtered for interpretation purpose and a moving average is used here to filter those high frequency variations. As expected, the initial states follow quite properly the theoretical distribution functions (Figure 11). The linearly initialized sea state then quickly moves toward a more nonlinear distribution both in crests and troughs values. The nonlinear initialized sea state is oscillating in the vicinity of the theoretical nonlinear distribution and generally presents a better agreement than the linearly initiated state in term of crest elevation, up to about 10Tp (Figure 12), when the differences become insignificant.

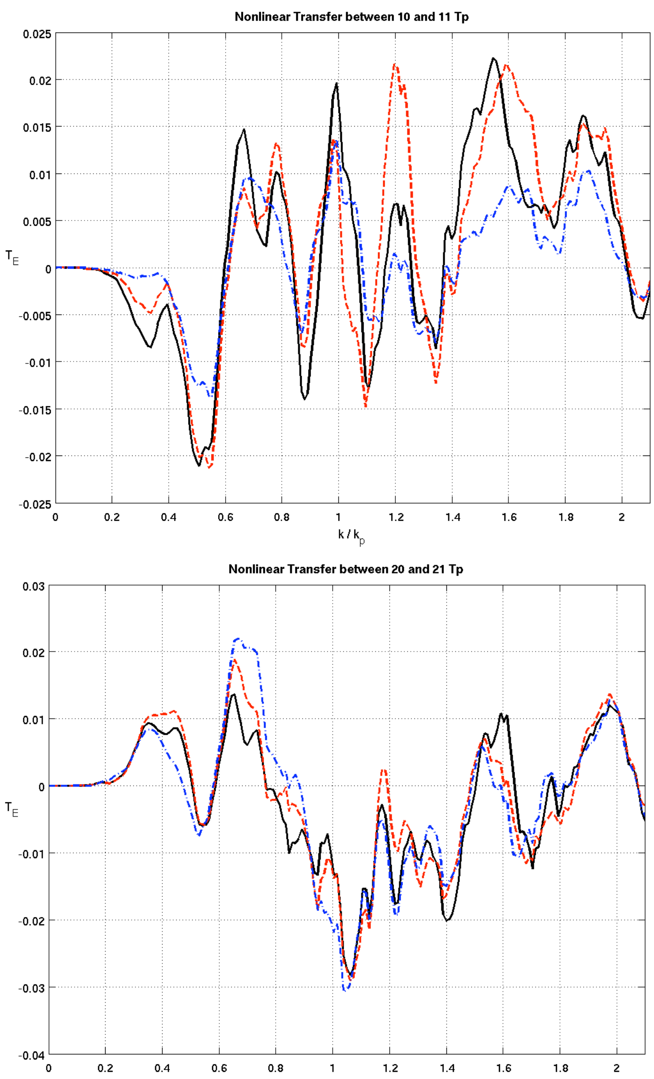

Figure 9 and Figure 10 - Integrated nonlinear transfers for second order non linear initialisation (black continuous), linear (red dashed) and relaxed (blue dash -dotted) initialization between 10 and 11 Tp and 20 and 21 Tp.

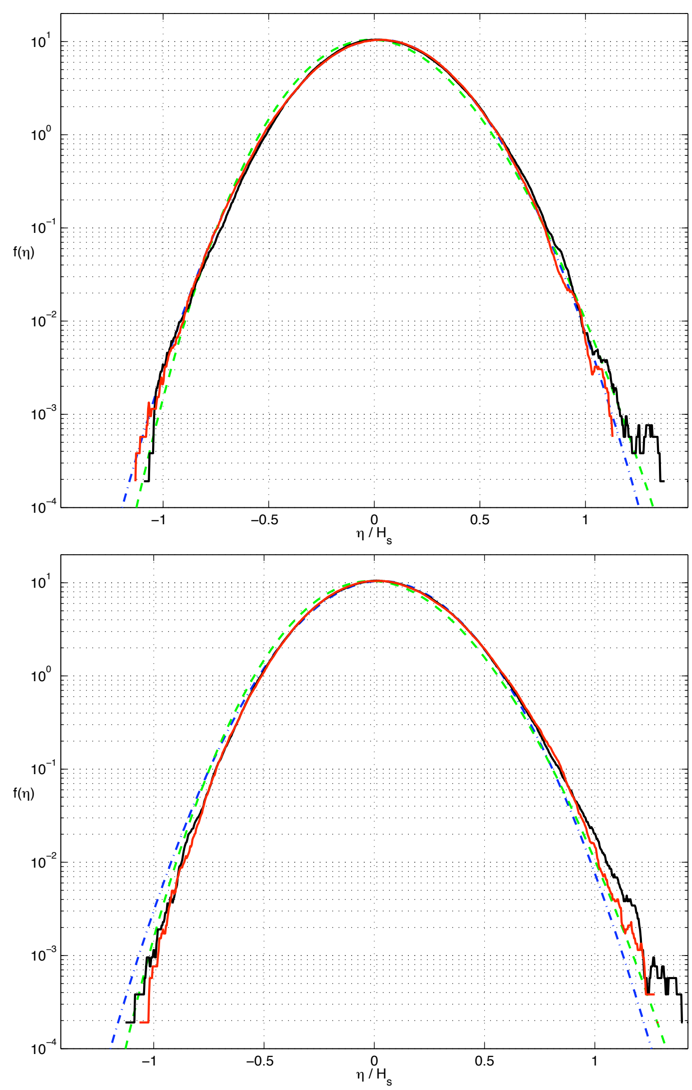

Figure 11 and Figure 12 - Initial distribution of surface elevation for linear set up (red), second order nonlinear set up (blue), theoritical Gauss linear (blue dash-dotted) and Tayfun nonlinear distribution (green dashed) at t=0 and t=10Tp

CONCLUSIONS

Three procedures of initialization for nonlinear sea state simulations have been tested on two different types of wave field.

Firstly bidimensional regular waves have been simulated at low order of nonlinearities (HOS simulations with M=2). When the simulation is initialized by a linear wave field, we observed spurious standing waves of amplitude up to two times the theoretical second order amplitude. The occurrence of those spurious waves has been explained by second order theory. Then a second order nonlinear initialization proved to significantly and immediately reduce the amplitude of those spurious components. The relaxation procedure proposed by Dommermuth(00) is able to provide a more accurate solution if enough time is allowed for the relaxation to occur.

Secondly we have performed tridimensional simulations of realistic sea states (irregular waves) with a higher order of nonlinearities (HOS model with M=3). This higher order of nonlinearity enables the spurious components to be dissipated through four waves interactions. Both linear and nonlinear initializations generate standing erroneous components during the first time steps, but the second order nonlinear initialization seems to provide a nonlinearly more relaxed sea state as suggested by integrated transfers and surface elevation statistics, in accordance with nonlinear theory. The relaxation procedure is able to damp spurious standing wave but implies however to provide the needed duration of relaxation. All three methods provide quite equivalent sea state after ten to twenty times the characteristic peak period.

ACKNOWLEDGMENTS

This study was achieved during a PHD work funded by the companies Actimar and Thales, at Laboratoire de Mecanique des Fluides in Ecole Centrale de Nantes.

REFERENCES

E. Blondel, G. Ducrozet, F. Bonnefoy, P. Ferrant. Extreme wave characterization and prediction using an advanced High-Order Spectral (HOS) model. *Proceedings of 27th Symposium on Naval Hydrodynamics.* 17 pages, 2008.

E. Blondel, G. Ducrozet, F. Bonnefoy et P. Ferrant. Deterministic reconstruction and prediction of a non-linear wave field using probe data. *Proceedings of OMAE'08*, 8 pages. 2008.

J.F. Dalzell. A note on finite depth second-order wave-wave interactions. *Applied Ocean Research*, 21:105 – 111, 1999.

D.G. Dommermuth. The initialization of nonlinear waves u sing an adjustment scheme. *Wave Motion*, 32:307 – 317, 2000.

D.G. Dommermuth, D.K.P. Yue. A high-order spectral method for the study of nonlinear gravity waves – *J. Fluid Mech.*, 184:267 – 288,1987.

F. Bonnefoy. G. Ducrozet, D. Le Touzé, P. Ferrant, Advances in Numerical Simulation of Nonlinear Water Waves, vol. 11 of *Advances in Coastal and Ocean Engineering*, chap. Time-Domain Simulation of Nonlinear Water Waves Using Spectral Methods, World Scientific, 2009.

K. Hasselman. On the non-linear energy transfer in a gravity-wave spectrum. Part1. General theory. *J. Fluid Mech.*, 12:481-500, 1962.

M.S. Longuet-Higgins. On the statistical distribution of the Heights of Sea Waves. *J. Marine Res.*, 11(3):245-266,1952.

M.A. Tayfun. Narrow-band nonlinear sea waves. *J. Geophysical Res.*, p1548-1552, 1980.

M. Tanaka. Verification of Hasselmann's energy transfer among surface gravity waves by direct simulations of primitive equations. . *J. Fluid Mech.*, 444:199 – 221, 2001.

B.J. West, K.A. Brueckner, R.S. Janda, M. Milder and R.L. Milton. A new numerical method for surface hydrodynamics. *J. Geophys. Res.*,92:11803 – 11824,1987.

APPENDIX A

THREE DIMENSIONAL SECOND ORDER NONLINEAR THEORY

`

Following Dalzell(99) the second order nonlinear sum and differences contributions for both φ_s and η are given by the following expressions :

$$A_+\left(\mathbf{k_{np}},\mathbf{k_{ij}}\right)=\frac{\omega_{np}\omega_{ij}\left(\omega_{np}+\omega_{ij}\right)\left[1-\cos\left(\theta_{np}-\theta_{ij}\right)\right]}{\left(\omega_{np}+\omega_{ij}\right)^2-g\left|\mathbf{k_{np}}+\mathbf{k_{ij}}\right|} \tag{34}$$

$$A_-\left(\mathbf{k_{np}},\mathbf{k_{ij}}\right)=\frac{\omega_{np}\omega_{ij}\left(\omega_{np}-\omega_{ij}\right)\left[1+\cos\left(\theta_{np}-\theta_{ij}\right)\right]}{\left(\omega_{np}-\omega_{ij}\right)^2-g\left|\mathbf{k_{np}}-\mathbf{k_{ij}}\right|} \tag{35}$$

for φ_s, and :

$$\begin{aligned}B_+\left(\mathbf{k_{np}},\mathbf{k_{ij}}\right)=&\frac{\left(\omega_{np}^2+\omega_{ij}^2\right)}{2g}\\&-\frac{\omega_{np}\omega_{ij}}{2g}\left[1-\cos\left(\theta_{np}-\theta_{ij}\right)\right]\left[\frac{\left(\omega_{np}+\omega_{ij}\right)^2+g\left|\mathbf{k_{np}}+\mathbf{k_{ij}}\right|}{\left(\omega_{np}+\omega_{ij}\right)^2-g\left|\mathbf{k_{np}}+\mathbf{k_{ij}}\right|}\right]\end{aligned} \tag{36}$$

$$\begin{aligned}B_-\left(\mathbf{k_{np}},\mathbf{k_{ij}}\right)=&\frac{\left(\omega_{np}^2+\omega_{ij}^2\right)}{2g}\\&+\frac{\omega_{np}\omega_{ij}}{2g}\left[1+\cos\left(\theta_{np}-\theta_{ij}\right)\right]\left[\frac{\left(\omega_{np}-\omega_{ij}\right)^2+g\left|\mathbf{k_{np}}-\mathbf{k_{ij}}\right|}{\left(\omega_{np}-\omega_{ij}\right)^2-g\left|\mathbf{k_{np}}-\mathbf{k_{ij}}\right|}\right]\end{aligned} \tag{37}$$

for η.

